

5-19-92  
E-6991

NASA Technical Memorandum 105679  
AIAA-92-3154

# An Experimental Investigation of High-Aspect-Ratio Cooling Passages

Julie A. Carlile  
*National Aeronautics and Space Administration*  
*Lewis Research Center*  
*Cleveland, Ohio*

and

Richard J. Quentmeyer  
*Sverdrup Technology, Inc.*  
*Lewis Research Center Group*  
*Brook Park, Ohio*

Prepared by the  
28th Joint Propulsion Conference  
cosponsored by the AIAA, SAE, ASME, and ASEE  
Nashville, Tennessee, July 6-8, 1992

**NASA**

# AN EXPERIMENTAL INVESTIGATION OF HIGH-ASPECT-RATIO

## COOLING PASSAGES

Julie A. Carlile  
National Aeronautics and Space Administration  
Lewis Research Center  
Cleveland, Ohio 44135

and

Richard J. Quentmeyer  
Sverdrup Technology, Inc.  
Lewis Research Center Group  
Brook Park, Ohio 44142

### Abstract

An experimental investigation was conducted to evaluate the effectiveness of using high-aspect-ratio cooling passages to improve the life and reduce the coolant pressure drop in high-pressure rocket thrust chambers. A plug-nozzle rocket-engine test apparatus was used to test two cylindrical chambers with low-aspect-ratio cooling passages and one with high-aspect-ratio cooling passages. The chambers were cyclically tested and data were taken over a wide range of coolant mass flows.

The results showed that for the same coolant pressure drop, the hot-gas-side wall temperature of the high-aspect-ratio chamber was 30 percent lower than the baseline low-aspect-ratio chamber, resulting in no fatigue damage to the wall. The coolant pressure drop for the high-aspect-ratio chamber was reduced in increments to one-half that of the baseline chamber, by reducing the coolant mass flow, and still resulted in a reduction in the hot-gas-side wall temperature when compared to the low-aspect-ratio chambers.

### Nomenclature

A cross sectional area  
C correlation coefficient  
C<sub>p</sub> specific heat  
D hydraulic diameter  
H heat transfer coefficient  
K conductivity

Pr Prandtl number  
Q heat flux  
Re Reynold's number  
T temperature  
W mass flow rate  
 $\mu$  viscosity  
 $\rho$  density

### Subscripts:

a adiabatic  
c coolant side  
g hot-gas side  
i integrated property  
s static  
w wall  
x reference

### Introduction

High pressure, reusable rocket engines, such as the SSME, are life limited due to cracks which form in the wall of the combustion-chamber liner. During engine operation, a large temperature difference exists between the hot-gas-side wall and the relatively cool structural

jacket, resulting in a high plastic strain in the hot-gas-side wall. This causes thinning and roughening of the hot-gas-wall with each thermal cycle, known as thermal ratcheting. After repeated thermal cycles, cracks develop in the wall.

One way to reduce this deleterious effect is to reduce the hot-gas-side wall temperature. Analyses have shown that the wall temperature can be reduced by substantially increasing the coolant-side surface area relative to the hot-gas-side surface area. This can be accomplished by increasing the number of cooling passages, which, for a given total coolant flow area, results in high-aspect-ratio cooling passages (generally, height/width > 4.0).

Another advantage of using high-aspect-ratio cooling passages is that it offers the potential of reducing the coolant pressure drop. For, if the wall temperature can be lowered substantially over that of a conventional design, less coolant would be required to cool the chamber resulting in a lower coolant velocity, and thus a lower pressure drop.

Although analyses have shown the merits of high-aspect-ratio cooling passages, the processes required to manufacture them had been lacking. Recently, improvements in manufacturing have shown that aspect ratios as high as eight can be manufactured by conventional means, and by using platelet technology, it has been demonstrated that chambers with aspect ratios as high as 15 can be manufactured.<sup>1</sup>

In order to evaluate this concept, an experimental investigation was conducted at NASA Lewis Research Center using the plug-nozzle rocket-engine test apparatus, which has been used extensively to evaluate advanced cooling concepts, candidate materials for thrust chamber liners, and techniques for improved manufacturing.<sup>2-7</sup> Three cylindrical chambers having aspect ratios at the throat of 0.75, 1.50, and 5.00 were tested. The chambers having aspect ratios of 0.75 and 1.50 are low-aspect-ratio cooling passages which are representative of conventional designs. For the high-aspect-ratio case, an aspect ratio of 5.00 was selected.

Cyclic hot-fire tests were conducted on the chambers at a nominal combustion chamber pressure of 4.136 MPa (600 psia) and a mixture ratio of 6.00 using gaseous hydrogen and liquid oxygen as propellants and liquid hydrogen as the coolant.

## Rocket Engine Test Apparatus

The test apparatus is a subscale plug-nozzle rocket-engine as shown in Fig. 1. It consists of an annular injector, a contoured centerbody which forms the chamber throat and nozzle sections, and an outer chamber which serves as the test section.

### Injector

The injector is designed to operate with liquid oxygen and gaseous hydrogen. The oxygen is injected through 70 tubes arranged in two circular rows, 36 in the inner row and 34 in the outer row. All of the fuel is injected through a porous face plate. Two chamber pressure taps, placed 180° apart, are located in the outer row of the oxidizer tubes.

### Centerbody

The water-cooled contoured centerbody is fabricated from copper with 40 rectangular cooling passages running axially throughout its length and is coated with ZrO<sub>2</sub>. The outside diameters of the combustion zone and the throat are 4.06- and 5.33-cm (1.6- and 2.1-in.), respectively. The centerbody is 15.24 cm (6.00 in.) in length with an expansion half-angle of 7.5°.

### Test Section Configurations

The chambers tested were made of OFHC copper and had an axial length of 15.24 cm (6.00 in.) and an inside diameter of 6.60 cm (2.6 in.). All the chambers had a wall thickness of 0.089 cm (0.035 in.) and were cooled with liquid hydrogen. The baseline configuration was designed to operate at a hot-gas-wall temperature of 778 K (1400 R) at a nominal coolant mass flow rate of 0.909 kg/s (2.0 lbm/s).<sup>2</sup> At these operating conditions the throat heat flux is approximately 97.1 MW/m<sup>2</sup> (33 Btu/in.<sup>2</sup>/s).

The combustion chamber configurations that were tested are given in Table 1. The baseline configuration had 72 axial cooling passages with an aspect ratio of 0.75. The second configuration had 100 cooling passages with an aspect ratio of 1.50. The third configuration had four bifurcations with 100, 200, and 400 cooling passages at various locations along its axial length as shown in Fig. 2. This was done to reduce the cooling passage surface area in the noncritical heat

transfer regions in order to minimize the overall pressure drop. The throat region had 400 cooling passages with an aspect ratio of 5.0. Figure 3 shows close-ups of the cross sections of the cooling passages in the three regions.

Due to the anticipated temperature reduction with increasing aspect ratio, the wall thickness could have been changed for each configuration. However, in order to make relative comparisons, the wall thickness for each configuration was kept constant.

#### Instrumentation

The cylindrical test sections were primarily instrumented with chromel/constantan thermocouples. Configurations 1 and 2 had eight thermocouples in the cooling passage ribs at alternating depths equally spaced around the circumference of the throat plane. Eight additional thermocouples were located on the backside wall between the rib thermocouples.

Configuration 3 had only backside thermocouples, since the cooling passage ribs were not wide enough to install rib thermocouples. There were eight thermocouples equally spaced around the circumference at the throat plane. Upstream of the throat, there were four additional backside thermocouples at both the 100- and 200-channel regions. Downstream of the throat, there were four thermocouples at the 200-channel region. In addition, all configurations had manifold inlet and outlet instrumentation to measure the coolant temperature and pressure.

#### Test Procedure

The tests were conducted in a 22 410-N (50 000-lb<sub>f</sub>) sea-level rocket test stand. The facility uses pressurized storage tanks to supply the propellents and coolant to the combustion chamber. Due to the small volume of the thrust chamber combustion zone, an external igniter was used to ignite the combustion chamber.

Cyclic hot-fire tests were conducted so that the heat-up portion of the cycle was long enough for the hot-gas side wall temperature to reach steady-state, and the chill-down portion of the cycle was long enough to bring the entire chamber back to liquid hydrogen temperature. Total cycle time was 3.5 s, 1.7 s of burn time and 1.8 s of chill-down time. The tests were conducted at a nominal chamber pressure of 4.136 MPa (600 psia) at an oxygen-to-fuel ratio of 6.0 using gaseous hydrogen and liquid oxygen as propellents.

In order to create the maximum thermal strain in the chamber wall, the liquid hydrogen flowed continuously for the entire cyclic test series. During the first cycle of any given test, a liquid hydrogen precool was used to bring the entire chamber to liquid hydrogen temperature prior to the ignition of the propellents. The chamber was considered to have failed when the first through crack appeared in the hot-gas wall, leaking coolant into the combustion chamber.

For configuration 1, the liquid hydrogen coolant flow rate was 0.841 kg/s (1.85 lbm/s) during burn time. The thrust chamber was continuously cycled until the supply of liquid hydrogen was depleted, approximately 70 cycles per tank of hydrogen. The tank was refilled, and cyclic tests continued until the chamber failed.

For configuration 2, the liquid hydrogen coolant flow rate was 0.886 kg/s (1.95 lbm/s) during burn time. Cyclic tests were performed as above for 295 cycles. Then, the chamber was tested at coolant flow rates of 0.841- and 0.750-kg/s (1.85- and 1.65-lbm/s) for approximately 10 cycles each, in order to obtain a wall temperature profile at various coolant flow rates. Cyclic tests continued with a coolant flow rate of 0.886 kg/s (1.95 lbm/s) until the chamber failed.

Configuration 3 was tested in the same manner as configuration 2. Due to the pressure drop increase, the coolant flow rate was set to the maximum attainable, 0.714 kg/s (1.57 lbm/s). The raw data indicated very low wall temperatures at this coolant mass flow. And after 340 thermal cycles, with no apparent fatigue damage to the wall, it was decided to determine the effect on wall temperature and coolant pressure drop of reduced coolant mass flows. So, the chamber was tested at the following coolant flow rates for approximately 10 cycles each: 0.641-, 0.600-, 0.559-, 0.495-, 0.400-, 0.314-, 0.255-, 0.182-kg/s (1.41-, 1.32-, 1.23-, 1.09-, 0.88-, 0.69-, 0.56-, and 0.40-lbm/s). After 440 cycles, the chamber still showed no damage due to thermal ratcheting, and testing was terminated.

#### Analysis

An analysis was performed to calculate the hot-gas wall temperature from the thermocouple data. The procedure for this is similar to the one outlined in Ref. 3. An in-house rocket engine heat transfer evaluation computer code (REHTEP) was used to determine the hot-gas and coolant side heat transfer coefficients and the hot-gas and coolant side adiabatic wall temperatures at the throat. These were then imported into a two-dimensional conduction analysis which used a

numerical differencing analyzer computer program (SINDA) to calculate the wall temperature profile at the throat.<sup>8</sup>

REHTEP calculated the hot-gas side heat transfer coefficient and heat flux by Eqs. (1) and (2), respectively.

$$H_g = \frac{C_g K_{gx} Re_{gx}^{0.8} Pr_{gx}^{0.33}}{D_g} \quad (1)$$

$$Q_g = H_g (T_{gaw} - T_{gw}) \quad (2)$$

The  $C_g$ 's along the axial length of the chamber were determined from a water-cooled calorimeter chamber of the same configuration.<sup>9</sup>

REHTEP assumes that the coolant is at a uniform bulk temperature at a given axial location and computes the coolant side heat transfer coefficient and heat flux by Eqs. (3) and (4), respectively.<sup>10</sup>

$$H_c = \frac{C_c W_c^{0.8} C_{p_{ci}}^{0.2} \mu_{ci}^{0.8} \rho_{ci}}{A_c^{0.8} D_c^{0.2} Pr_{ci}^{0.6} \rho_{cs}^{0.8}} * ent \quad (3)$$

$$Q_c = H_c \sigma (T_{cw} - T_{caw}) \quad (4)$$

where  $C_c = 0.023$ ,  $ent$  is an entrance effect, and  $s$  is a two-dimensional fin approximation dependent on the channel geometry, material conductivity, and coolant heat transfer coefficient.<sup>10</sup>

The code varies the wall temperature until  $Q_g = Q_c$ . REHTEP accounts for the thrust chamber geometry, cooling passage inlet temperature and pressure, the coolant mass flow, and the chamber pressure. Once the heat transfer coefficients and adiabatic wall temperatures at the throat section were determined, they are used as input variables into the two-dimensional conduction analysis.

Figures 4(a), (b), and (c) are cross section schematics of half a cooling passage showing the nodes for the numerical differencing analysis for configurations 1, 2, and 3, respectively. Also, indicated in Fig. 4 are the locations of the adiabatic wall temperatures and the heat transfer coefficients. As shown, three different coolant side heat transfer coefficients ( $H_{c1}$ ,  $H_{c2}$ , and  $H_{c3}$ ) were used along the cooling passage wall. The

coolant side heat transfer coefficient calculated from REHTEP was used for  $H_{c1}$ , while  $H_{c2}$  and  $H_{c3}$  were adjusted accordingly to make the best fit of the thermocouple data.

## Results and Discussion

The objective of this program was to evaluate the effectiveness of using high-aspect-ratio cooling passages to improve the life and reduce the coolant pressure drop in high-pressure rocket thrust chambers.

Figure 5 shows photos of the hot-gas wall at the throat section after testing for the three configurations. Progressive fatigue damage was observed in configurations 1 and 2 (Figs. 5(a) and (b)) throughout the cyclic testing, with wall cracks developing at 200 and 590 thermal cycles, respectively. No fatigue damage was observed in configuration 3 (Fig. 5(c)), even after 440 cycles, thus testing was terminated. See Table 2 for a comparison of the chamber life for the three configurations tested.

In order to show the effects of temperature on the grain structure in the wall after testing, cross sections of the throat wall were polished and etched, and microphotographs were taken (Fig. 6). For configurations 1 and 2 (Figs. 6(a) and (b)), there was metal movement and recrystallization due to the high strain and temperature they were exposed to. The small recrystallized grains, which also have annealing twins at the hot-gas side surface, indicate that the material on the hot-gas side was at a temperature approximately 700 to 810 K (1260 to 1450 R) or greater. The thinning of the cooling passage wall, the doghouse shape, and the through crack are typical of failures due to thermally induced plastic ratcheting. Configuration 3 (Fig. 6(c)), on the other hand, had no grain size change or material movement indicating that the hot-gas wall was below 700 to 810 K (1260 to 1450 R).<sup>7</sup> Furthermore, the chamber wall appearance remained in the as-fabricated condition as shown in Figs. 5(c) and 6(c).

Figures 7, 8, and 9 show the SINDA node and experimental wall temperatures for configurations 1, 2, and 3, respectively. For configurations 1 and 2, the node temperatures along the cooling passage rib centerline were matched with the thermocouple data (Figs. 7 and 8, respectively). The plot for configuration 1 is given at a coolant mass flow rate of 0.841 kg/s (1.85 lbm/s). Plots are given for configuration 2 at coolant mass flow rates of 0.909-, 0.841-, and 0.773-kg/s (2.00-, 1.85-, and 1.70-lbm/s) (Figs. 8(a), (b), and (c)). Only backside node temperatures could be matched to the thermocouple data for configuration 3

so the temperature of the backside wall is plotted as a function of coolant mass flow. Figure 10 gives a typical contoured plot produced by the two-dimensional conduction analysis showing the temperature profile in the chamber wall for the baseline configuration.

As shown in Fig. 10, the highest wall temperature was located on the cooling passage centerline at the hot-gas-side wall. This wall temperature was plotted as a function of aspect ratio for a coolant pressure drop of (600 psid) (Fig. 11). As the aspect ratio increased from 0.75 to 5.00, the hot-gas-side wall temperature decreased from 765 to 539 K (1377 to 970 R) showing a significant reduction in wall temperature (here 30 percent) with increasing aspect ratio. In addition, the data indicate that a significant further reduction in the hot-gas-side wall temperature could have been achieved by using aspect ratios greater than 5.00. This shows the effectiveness of increasing the coolant side surface area relative to that of the hot-gas side.

Plots of the hot-gas wall temperature are given as a function of coolant mass flux (Fig. 12) and coolant pressure drop (Fig. 13) at the various aspect ratios. Mass flux was used as opposed to mass flow rate, because there were variations in the overall coolant passage flow area between the chambers. The data shows that even at reduced coolant pressure drops (achieved by reducing the coolant mass flow) the high-aspect ratio passages provide a significant reduction in wall temperature. Here the coolant pressure drop for the high-aspect-ratio chamber was reduced in increments to approximately one-half that of the baseline chamber, and there was still a 5.2 percent reduction in the hot-gas-side wall temperature [from 765 to 725 K (1377 to 1305 R)].

#### Summary of Results

An investigation was conducted to determine the effectiveness of using high-aspect-ratio cooling passages to improve the life and reduce the coolant pressure drop in high-pressure rocket thrust chambers. Three cylindrical chambers were cyclically tested using a subscale plug-nozzle rocket-engine test apparatus. Each chamber had a different aspect ratio and number of cooling passages. The following results were determined:

1. The chamber with the high-aspect-ratio (5.00) cooling passages showed no fatigue damage to the hot-gas-side wall after 440 thermal cycles indicating a substantial increase in chamber life over the low-aspect-ratio (0.75 and 1.50) chambers, which sustained severe wall damage due to thermal ratcheting, resulting in wall cracks.

2. For the same coolant pressure drop as in the baseline chamber, the high-aspect-ratio chamber showed a 30-percent reduction in the hot-gas-side wall temperature.

3. The coolant pressure drop for the high-aspect-ratio chamber was reduced in increments to one-half that of the baseline chamber, by reducing the coolant mass flow, and still resulted in a reduction in the hot-gas-side wall temperature.

4. The data indicate that the hot-gas-side wall temperatures for the high-aspect-ratio chamber could have been reduced substantially further by using aspect ratios greater than 5.00.

#### Conclusion

The use of high-aspect-ratio cooling passages in the design of high-pressure rocket thrust chambers has the potential of significantly increasing chamber life as a result of lower wall temperatures. And at the same time the power requirements for the turbomachinery can be reduced as a result of lower coolant pressure drop.

#### Concluding Remarks

It should be noted that the data presented in this report were obtained in straight cooling passages. The effect on the curvature-enhancement factor in the throat region of contoured rocket chambers has yet to be determined for high-aspect-ratio cooling passage designs. In addition, due to the reduction in the hot-gas wall temperature by using high-aspect-ratio cooling passages, the wall could be made thinner which would result in a further reduction of the hot-gas-side wall temperature.

The effectiveness of high-aspect-ratio cooling passages is a function of the heat flux level and the amount of mixing which occurs in the coolant between the bottom and the top of the cooling passages. Therefore, the optimum aspect ratio would be different for each combustion chamber application.

#### References

1. Tobin, S., Mueggenburg, H., Burkhardt, W., "Formed Platelet Liner Concept for Regeneratively Cooled Chambers," AIAA Paper 90-2117, July 1990.

2. Quentmeyer, R.J., "Experimental Fatigue Life Investigation of Cylindrical Thrust Chambers," AIAA Paper 77-893, July 1977.
3. Quentmeyer, R.J., "Thrust Chamber Thermal Barrier Coating Techniques," NASA TM-100933, 1988.
4. Quentmeyer, R.J., Kasper, H.J., and Kazaroff, J.M., "Investigation of the Effect of Ceramic Coatings on Rocket Thrust Chamber Life," NASA TM-78892, 1978.
5. Kazaroff, J.M., Jankovsky, R.S., Pavli, A.J. "Hot Fire Test Results of Subscale Tubular Combustion Chambers," To be published as NASA TP-3222, 1992.
6. Kazaroff, J.M., and Jankovsky, R.S., "Cyclic Hot Firing of Tungsten-Wire Reinforced, Copper-Lined Thrust Chambers," NASA TM-4214, 1990.
7. Pavli, A.J., Kazaroff, J.M., and Jankovsky, R.S., "Hot Fire Fatigue Testing Results For the Compliant Combustion Chamber," To be published as NASA TP-3223, 1992.
8. Smith, J.P., "Systems Improved Numerical Differencing Analyzer (SINDA): User's Manual," (TRW-14690-H001-R0-00, TRW Systems Group; NASA Contract NAS9-10435) NASA CR-134271, 1971.
9. Roncace, E.A., and Quentmeyer, R.J., "Hot-Gas-Side Heat-Transfer Characteristics of a Subscale Plug-Nozzle Rocket Test Apparatus," To be published as NASA TM-158241, 1992.
10. Schacht, R.L., and Quentmeyer, R.J., "Coolant-Side Heat-Transfer Rates For a Hydrogen-Oxygen Rocket and a New Technique For Data Correlation," NASA TN D-7207, 1973.

Table 1.—Combustion Chamber Configurations

Configuration	Aspect ratio (throat)	Number of passages (throat)	Channel height (throat)	Channel width (throat)
1 (Baseline)	0.75	72	0.127 cm (0.050 in.)	0.170 cm (0.067 in.)
2	1.50	100	0.152 cm (0.060 in.)	0.102 cm (0.040 in.)
3	5.00	400	0.127 cm (0.050 in.)	0.0254 cm (0.010 in.)

Table 2.—Comparison of Chamber Life

Configuration	Aspect ratio	Life (cycles)	Fatigue damage
1 (Baseline)	0.75	200	Progressive
2	1.50	590	Progressive
3	5.00	No failure at 440 cycles	None

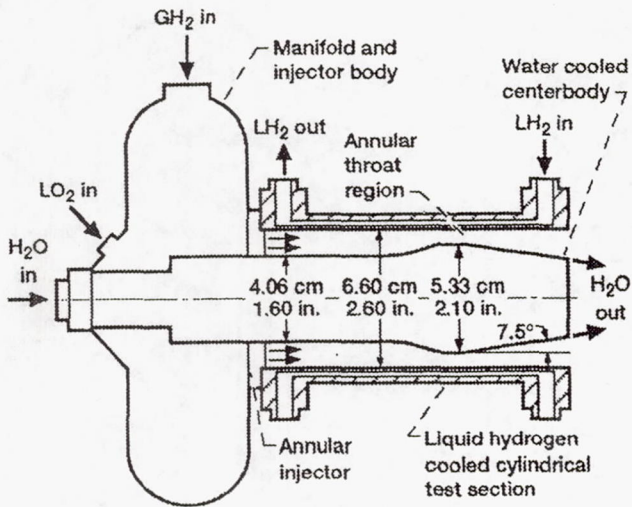


Figure 1.—Subscale rocket engine test apparatus.

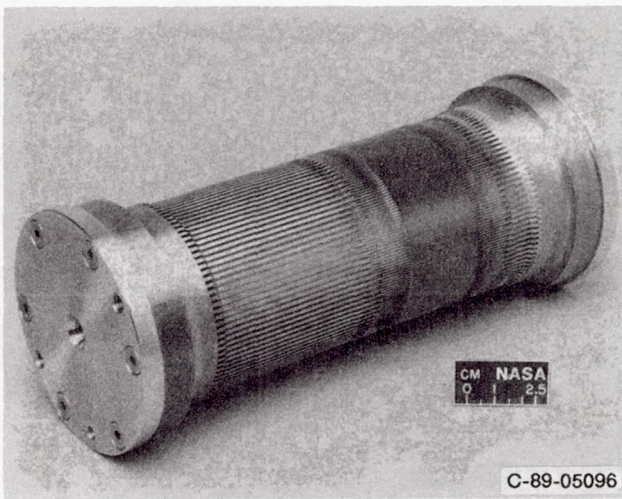
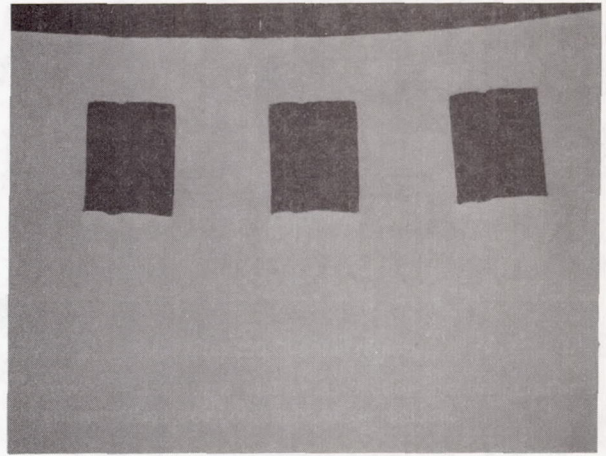
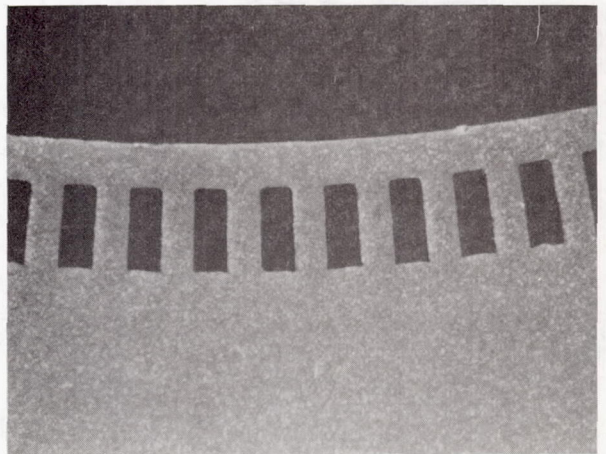


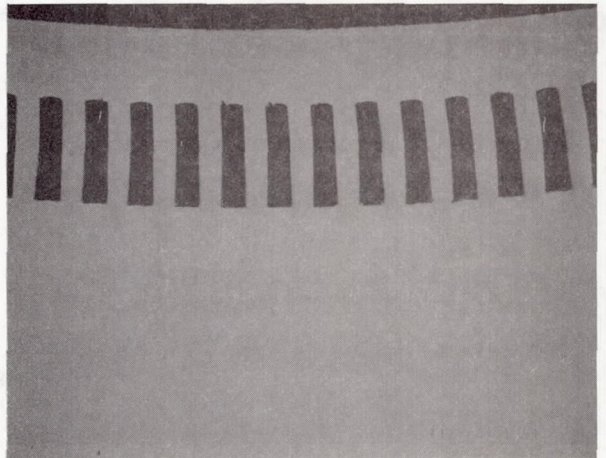
Figure 2.—High aspect ratio chamber liner.



(a) 100 Channel region.



(b) 200 Channel region.



(c) 400 Channel region.

Figure 3.—Close-up of wall cross-section for configuration 3 showing the three cooling passage regions.

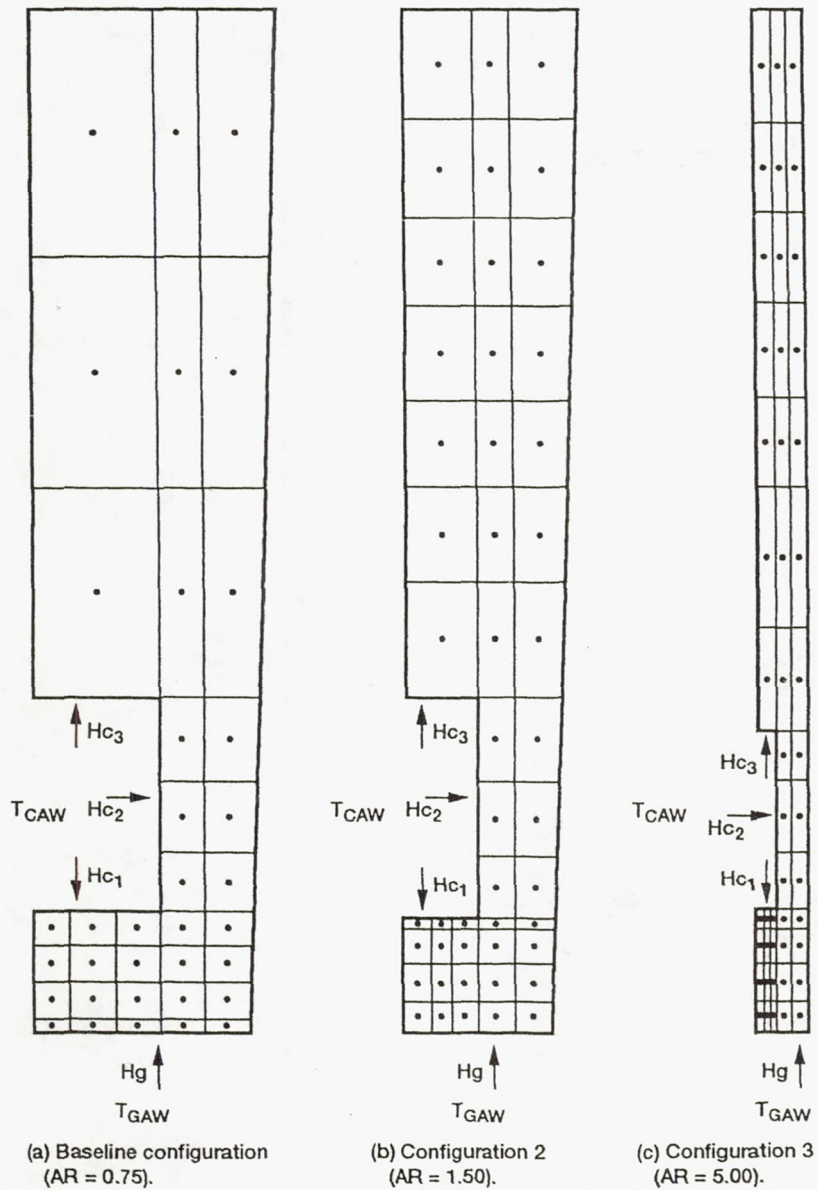
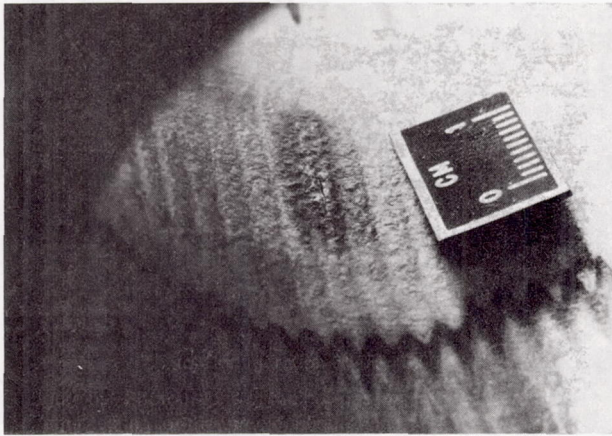


Figure 4.—Cooling passage models used for SINDA analysis.



(a) Baseline configuration (AR = 0.75).

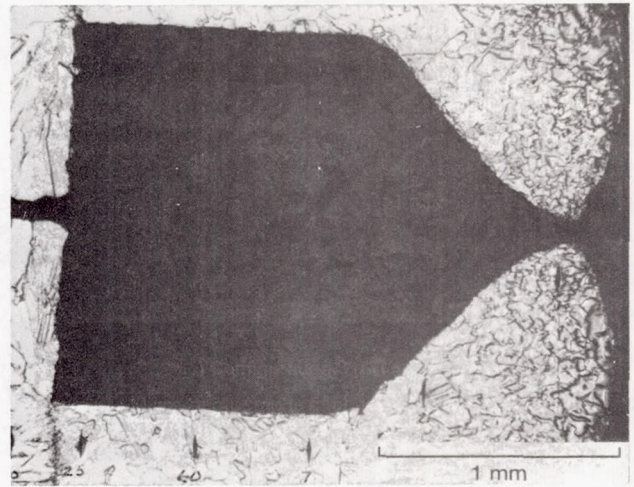


(b) Configuration 2 (AR = 1.50).

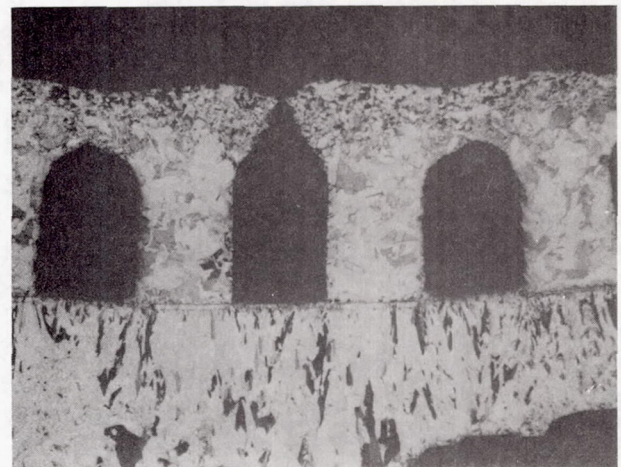


(c) Configuration 3 (AR = 5.00).

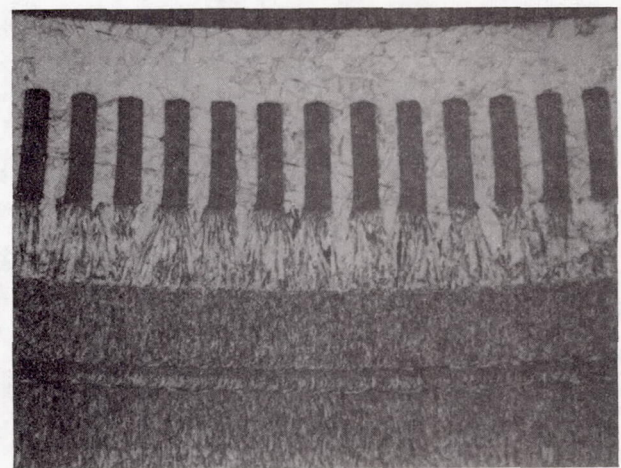
Figure 5.—Photographs of the hot-gas wall at the throat section after testing for the three configurations.



(a) Baseline configuration (AR = 0.75).



(b) Configuration 2 (AR = 1.50).



(c) Configuration 3 (AR = 5.00).

Figure 6.—Micro-photographs of chamber wall cross-section at the throat.

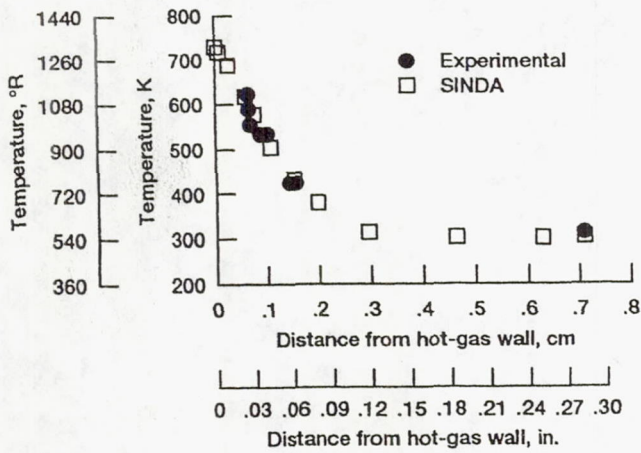


Figure 7.—SINDA analysis and experimental wall temperatures along the centerline of the cooling passage rib for configuration 1.

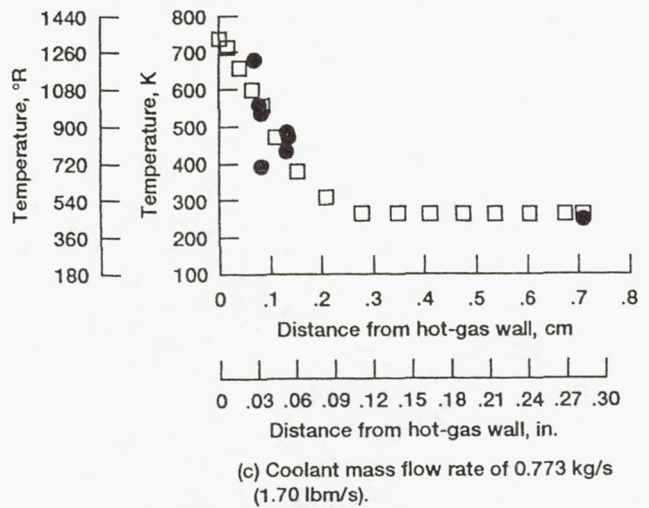
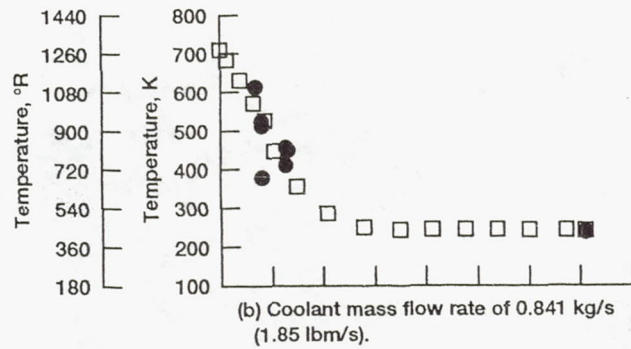
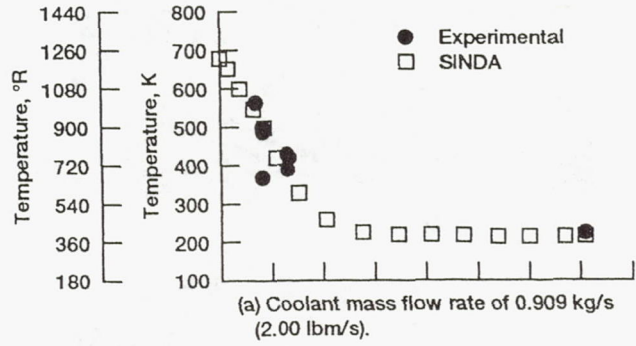


Figure 8.—SINDA analysis and experimental wall temperatures along the centerline of the cooling passage rib for configuration 2.

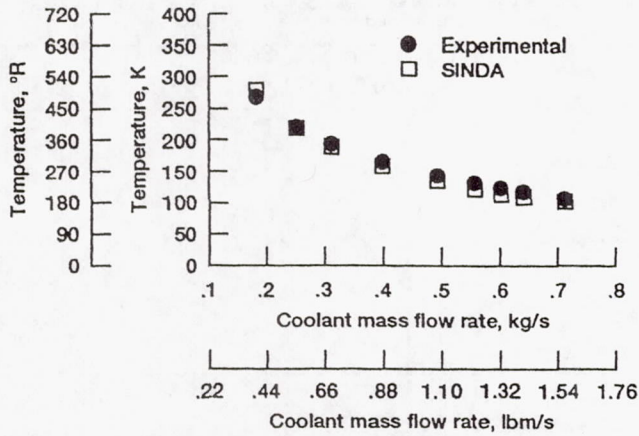


Figure 9.—Experimental and SINDA analysis backside wall temperatures as a function of coolant flow rate for configuration 3.

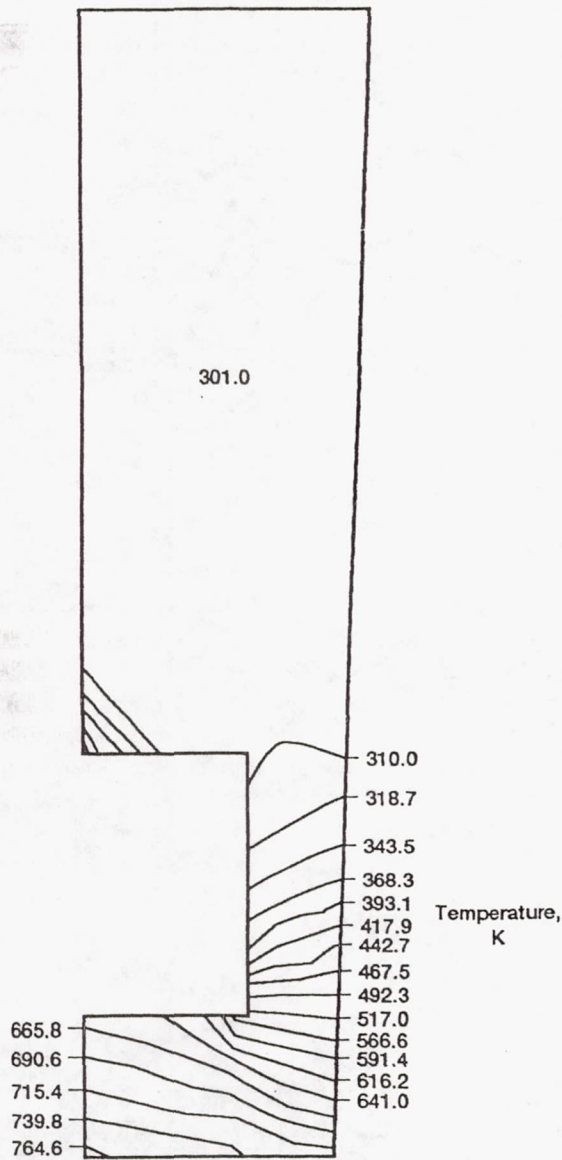


Figure 10.—Temperature profile produced by the two-dimensional conduction analysis for the baseline configuration (AR = 0.75).

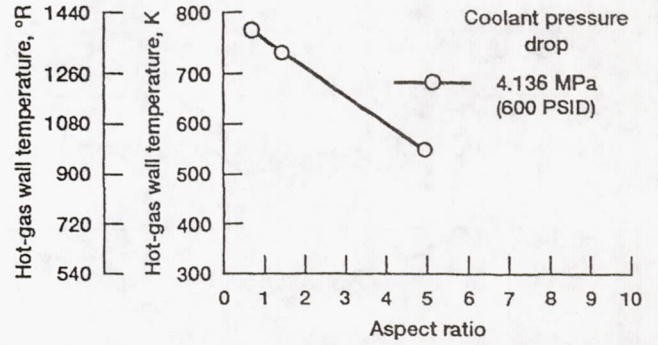


Figure 11.—Hot-gas-side wall temperature versus aspect ratio at a coolant pressure drop of 4.136 MPa (600 PSID).

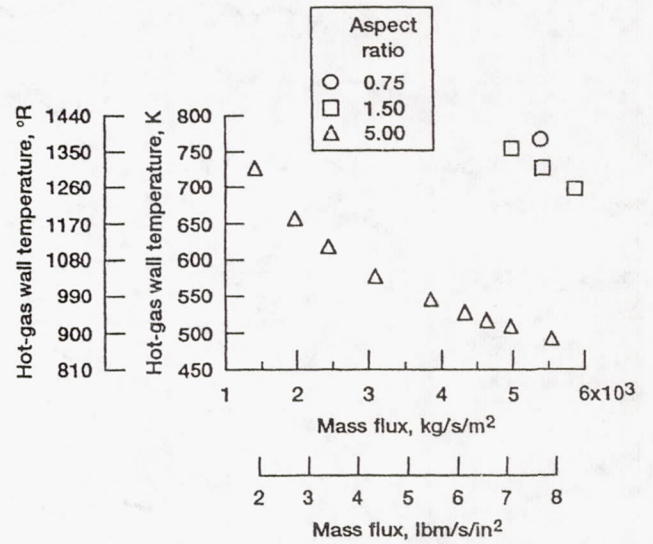


Figure 12.—Hot-gas wall temperature versus coolant mass flux.

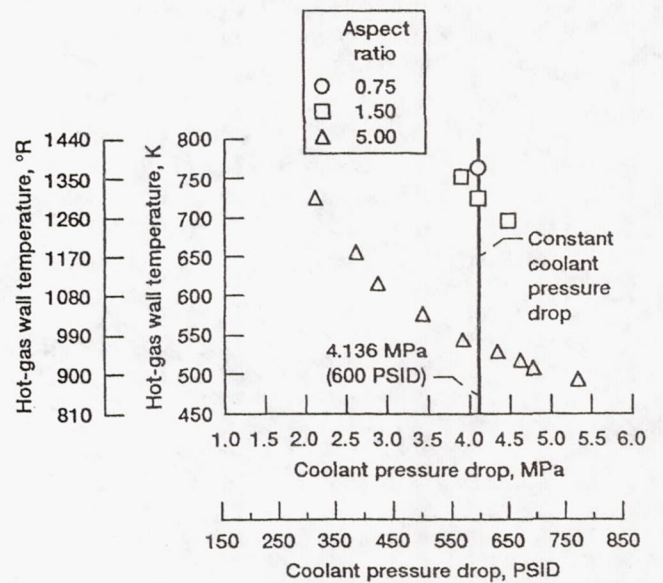


Figure 13.—Hot-gas wall temperature versus coolant pressure drop.

**REPORT DOCUMENTATION PAGE**Form Approved  
OMB No. 0704-0188

Public reporting burden for this collection of information is estimated to average 1 hour per response, including the time for reviewing instructions, searching existing data sources, gathering and maintaining the data needed, and completing and reviewing the collection of information. Send comments regarding this burden estimate or any other aspect of this collection of information, including suggestions for reducing this burden, to Washington Headquarters Services, Directorate for Information Operations and Reports, 1215 Jefferson Davis Highway, Suite 1204, Arlington, VA 22202-4302, and to the Office of Management and Budget, Paperwork Reduction Project (0704-0188), Washington, DC 20503.

<b>1. AGENCY USE ONLY (Leave blank)</b>		<b>2. REPORT DATE</b> July 1992	<b>3. REPORT TYPE AND DATES COVERED</b> Technical Memorandum	
<b>4. TITLE AND SUBTITLE</b> An Experimental Investigation of High-Aspect-Ratio Cooling Passages			<b>5. FUNDING NUMBERS</b>  WU-590-21-11	
<b>6. AUTHOR(S)</b> Julie A. Carlile and Richard J. Quentmeyer				
<b>7. PERFORMING ORGANIZATION NAME(S) AND ADDRESS(ES)</b>  National Aeronautics and Space Administration Lewis Research Center Cleveland, Ohio 44135-3191			<b>8. PERFORMING ORGANIZATION REPORT NUMBER</b>  E-6991	
<b>9. SPONSORING/MONITORING AGENCY NAMES(S) AND ADDRESS(ES)</b>  National Aeronautics and Space Administration Washington, D.C. 20546-0001			<b>10. SPONSORING/MONITORING AGENCY REPORT NUMBER</b>  NASA TM-105679 AIAA-92-3154	
<b>11. SUPPLEMENTARY NOTES</b>  Prepared for the 28th Joint Propulsion Conference cosponsored by the AIAA, SAE, ASME, and ASEE, Nashville, Tennessee, July 6-8, 1992. Julie A. Carlile, NASA Lewis Research Center and Richard J. Quentmeyer, Sverdrup Technology, Inc., Lewis Research Center Group, 2001 Aerospace Parkway, Brook Park, Ohio 44142. Responsible person, Julie A. Carlile, (216) 433-7431.				
<b>12a. DISTRIBUTION/AVAILABILITY STATEMENT</b>  Unclassified - Unlimited Subject Category 15			<b>12b. DISTRIBUTION CODE</b>	
<b>13. ABSTRACT (Maximum 200 words)</b>  An experimental investigation was conducted to evaluate the effectiveness of using high-aspect-ratio cooling passages to improve the life and reduce the coolant pressure drop in high-pressure rocket thrust chambers. A plug-nozzle rocket-engine test apparatus was used to test two cylindrical chambers with low-aspect-ratio cooling passages and one with high-aspect-ratio cooling passages. The chambers were cyclically tested and data were taken over a wide range of coolant mass flows. The results showed that for the same coolant pressure drop, the hot-gas-side wall temperature of the high-aspect-ratio chamber was 30 percent lower than the baseline low-aspect-ratio chamber, resulting in no fatigue damage to the wall. The coolant pressure drop for the high-aspect-ratio chamber was reduced in increments to one-half that of the baseline chamber, by reducing the coolant mass flow, and still resulted in a reduction in the hot-gas-side wall temperature when compared to the low-aspect-ratio chambers.				
<b>14. SUBJECT TERMS</b> Rocket combustors; Rocket engine cooling; Aspect ratio; Chamber liner			<b>15. NUMBER OF PAGES</b> 12	
			<b>16. PRICE CODE</b> A03	
<b>17. SECURITY CLASSIFICATION OF REPORT</b> Unclassified	<b>18. SECURITY CLASSIFICATION OF THIS PAGE</b> Unclassified	<b>19. SECURITY CLASSIFICATION OF ABSTRACT</b> Unclassified	<b>20. LIMITATION OF ABSTRACT</b>	



National Aeronautics and  
Space Administration

**Lewis Research Center**  
Cleveland, Ohio 44135

Official Business  
Penalty for Private Use \$300

**FOURTH CLASS MAIL**

ADDRESS CORRECTION REQUESTED



Postage and Fees Paid  
National Aeronautics and  
Space Administration  
NASA 451

**NASA**

---